Supplementary information for

Definition of an Antibody-Dependent Cellular Cytotoxicity (ADCC) Response Implicated in Reduced Risk for HIV-1 Infection

Priyamvada Acharya[1], William D. Tolbert[2,3], Neelakshi Gohain[2,3], Xueji Wu[2,3], Lei Yu[2,4], Tongyun Liu[2,4], Wensheng Huang [2,4], Chih-chin Huang[1], Young Do Kwon[1], Robert K. Louder[1], Timothy S. Luongo[1], Jason S. McLellan[1], Marie Pancera[1], Yongping Yang[1], Baoshan Zhang[1], Robin Flinko[2,4], James S Foulke, Jr.[2,5], Mohammad M. Sajadi[2,5,6], Roberta Kamin-Lewis[2,4], James E. Robinson[7], Loïc Martin[8], Peter D. Kwong[1], Yongjun Guan[2,4], Anthony L. DeVico[2,5], George K. Lewis[2,4], Marzena Pazgier[2,3*]

[1]Vaccine Research Center, National Institute of Allergy and Infectious Diseases, National Institutes of Health, Bethesda, MD 20892, USA

[2]Institute of Human Virology and Departments of [3]Biochemistry and Molecular Biology, [4]Microbiology and Immunology and [5]Medicine of University of Maryland School of Medicine, Baltimore, MD 21201, USA

[6]Medical Care Clinical Center, VA Maryland Health Care Center, Baltimore, MD 21201, USA

[7]Department of Pediatrics, Tulane University Medical Center, New Orleans, LA 70112, USA

[8]CEA, iBiTecS, Service d'Ingénierie Moléculaire des Protéines, F-91191 Gif-sur-Yvette, France

*To whom correspondence should be addressed:

Email: mpazgier@ihv.umaryland.edu

725 West Lombard Street, Baltimore, MD 21201, USA

Tel: (410)706-4780

Fax: (410)706-7583

Supplemental Tables

Table S1. Crystallographic data collection and refinement statistics.

	Crystal				
	Fab N5-i5-gp120$_{93TH057}$-*d1d2*CD4	Fab 2.2c	Fab 2.2c-gp120$_{89.6P}$ -*d1d2*CD4	Fab 2.2c-gp120$_{YU2}$-M48U1	Fab 2.2c-gp120$_{92UG037}$-M48U1
Data collection					
Wavelength, Å	0.979	1.000	1.000	1.000	1.000
Space group	$P2_12_12_1$	$C2_1$	$P2_12_12_1$	F222	P1
Cell parameters					
a, b, c, Å	92.3, 103.9, 134.7	195.0, 133.6, 90.8	61.4, 69.4, 328.6	158.3, 171.2, 228.0	113.0, 144.2, 158.4
α, β, γ, °	90, 90, 90	90, 91.4, 90	90, 90, 90	90, 90, 90	110.6, 92.3, 99.2
Complexes/a.u.	1	4	1	1	8
Resolution, (Å)	50-1.85 (1.88-1.85)	50-2.20 (2.28-2.20)	50-4.28 (4.90-4.28)	50-3.5 (3.63-3.50)	50-3.78 (4.07-3.78, 3.78-3.56)
# of reflections					
Total	825,392	382614	12,216	94,677	161,599
Unique	110,501	110015	7941	13,957	71,903
R_{merg}[b], %	6.4 (83.1)	9.0 (40)	5.2 (36.1)	7.3 (52.3)	9.6 (27.6, 26.2)
I/σ	45.0 (2.9)	12.6 (2.0)	30.0 (2.0)	10.9 (2.0)	28.2 (2.4, 1.8)
Completeness, %	100 (99.9)	93.6 (67.8)	76.8 (65.0)	85.7 (59.5)	70.2 (52.3, 37.5)
Redundancy	7.5 (7.4)	3.5 (2.3)	6.5 (2.4)	5.4 (1.9)	2.2 (1.8, 1.5)
Refinement Statistics					
Resolution, Å	41.2-1.85	48.6-2.20	47.7-4.28	35.5-3.50	49.1-3.56
R[c], %	17.7	18.1	31.1	26.0	30.6
R_{free}[d], %	21.1	22.4	32.1	29.8	32.4
# of atoms					
Protein	7,156	13054	7,415	6,219	47,564
Water	762	1233	0	0	0
Ligand/Ion	170	236	0	2	0
Overall B value $(Å)^2$					
Protein	41.5	41.7	162	188.6	120.3
Water	44.3	44.6	NA	NA	NA
Ligand/Ion	57.7	82.1	NA	192.0	NA
Root mean square deviation					
Bond lengths, Å	0.007	0.003	0.007	0.004	0.007
Bond angles, °	1.21	0.92	0.823	1.004	1.02
Ramachandran[e]					
favored, %	96.9	96.0	91.2	97.4	91
allowed, %	2.5	3.76	8.2	2.4	8.0
outliers, %	0.6	0.24	0.6	0.2	1.0
PDB code	4H8W	4R4B	4R4H	4R4F	4R4N

Values in parentheses are for highest-resolution shell

[b] $R_{merge} = \sum | I - \langle I \rangle | / \sum I$, where I is the observed intensity and $\langle I \rangle$ is the average intensity obtained from multiple observations of symmetry-related reflections after rejections

[c] $R = \sum \| F_o | - | F_c \| / \sum | F_o |$, where F_o and F_c are the observed and calculated structure factors, respectively

[d] R_{free} = defined by by Brünger (1)

[e] Calculated with MolProbity (2)

Table S2. **Interactions at the 2.2c-gp120 interfaces.** Accessible Surface Area, Å² (**ASA**) and Buried Surface Area, Å² (**BSA**) were calculated for each of three 2.2c fab complexes using the EBI PISA server (http://www.ebi.ac.uk/msd-srv/prot_int/cgi-bin/piserver. Residues contributing to the interface through H bonds

2.2c-gp120$_{89.6P}$ dV1V2

Heavy Chain		ASA	BSA
CDR H1	H:GLY 31	46.96	13.95 |||
	H:TYR 33[H]	58.66	40.37 |||||||
CDR H2	H:TRP 47	76.31	10.97 ||
	H:GLU 50	17.63	8.67 |||||
	H:LYS 52[HS]	54.63	30.96 ||||||
	H:SER 56	69.81	16.25 |||
	H:PRO 57[H]	60.96	24.55 |||||
	H:ASN 58[H]	80.61	59.47 |||||||
	H:TYR 59[H]	47.85	25.01 ||||||
	H:PRO 61	116.2	49.76 |||||
	H:LYS 64	144.5	44.29 ||||
CDR H3	H:ARG 95	36.71	21.95 ||||||
	H:ASN 97[H]	98.76	53.14 |||||||
	H:TRP 98	197.55	180.43 ||||||||||
	H:PRO 99	101.2	27.27 |||
	H:LEU 100A	76.74	26.61 ||||

gp120$_{89.6}$		ASA	BSA
Layer 1	A:PHE 53	139.91	28.32 |||
	A:CYS 54	12.87	3.31 |||
	A:ASP 57	121.01	14.88 ||
	A:ALA 58	25.81	14.96 ||||||
	A:LYS 59	96.84	23.07 |||
	A:ALA 60[H]	75.56	56.68 |||||||
	A:TYR 61[H]	163.3	134.21 ||||||||
	A:THR 63	114.85	4.36 |
	A:THR 71	65.58	5.31 |
	A:VAL 75	91.72	62.16 |||||||
	A:PRO 76[H]	93.68	57.27 |||||||
	A:THR 77[H]	64.92	59.08 |||||||||
	A:ASP 78[HS]	97.44	36.12 ||||
Layer 2	A:PRO 79	76.63	27.50 ||||
	A:ASN 80	123.45	31.66 |||
	A:CYS 218	11.44	11.27 |||||||||
	A:VAL 219	5.83	3.20 ||||||
	A:PRO 220	36.16	11.94 ||||
	A:ALA 221	103.85	14.94 ||
	A:GLN 246	95.86	23.85 |||
	A:CYS 247	24.94	1.65 |

Light Chain		ASA	BSA
	L:ILE 2	36.15	17.98 |||||
CDR L1	L:GLN 27	95.37	6.12 |
	L:GLY 28	60.23	10.07 ||
	L:ILE 29	8.23	0.84 ||
	L:SER 30	60.06	0.91 |
CDR L3	L:TYR 32	99.49	58.03 ||||||
	L:HIS 90	11.98	8.11 |||||||
	L:ILE 92	66.98	57.97 ||||||||
	L:GLY 93[H]	51.27	43.85 ||||||||
	L:LEU 94	126.75	11.85 |
	L:ARG 96	131.47	42.09 ||||

gp120$_{89.6}$		ASA	BSA
Layer 1	A:PHE 53	139.91	34.90 |||
	A:ALA 60	75.56	18.88 |||
	A:THR 71[H]	65.58	49.65 |||||||
	A:HIS 72	151.68	92.08 |||||||
	A:ALA 73	45.06	11.61 |||
	A:CYS 74	22.45	17.09 |||||||
	A:VAL 75	91.72	29.55 ||||
	A:PRO 76	93.68	17.24 ||

2.2c-gp120$_{YU2}$ core$_e$

Heavy chain		ASA	BSA
CDR H1	H:GLY 31	27.74	1.82 |
	H:TYR 33 [H]	56.56	45.54 ||||||||
CDR H2	H:GLU 50	21.38	12.03 ||||||
	H:LYS 52 [HS]	51.99	37.95 |||||||
	H:HIS 53	71.3	10.01 ||
	H:ASN 54	98.29	1.60 |
	H:SER 56	61.38	17.23 |||
	H:PRO 57 [H]	66.51	26.93 |||||
	H:ASN 58 [H]	79.47	59.10 |||||||
	H:TYR 59	46.83	25.65 ||||||
	H:HIS 60	45.89	2.19 |
	H:PRO 61	118.22	46.20 ||||
	H:LYS 64	153.02	39.17 |||
CDR H3	H:ARG 95	31.84	19.92 ||||||
	H:ASN 97 [H]	78.47	50.55 ||||||
	H:TRP 98	203.68	187.28 |||||||||
	H:PRO 99	90.37	1.67 |
	H:LEU 100A	94.16	26.60 |||

gp120 $_{YU2}$		ASA	BSA
Layer 1	G:PHE 53	126.63	17.17 ||
	G:ASP 57	127.88	25.46 ||
	G:ALA 58 [H]	24.45	16.67 ||||||
	G:LYS 59 [H]	94.44	33.74 ||||
	G:ALA 60 [H]	96.5	62.21 ||||||
	G:TYR 61	167.74	141.68 ||||||||
	G:THR 71	51.8	1.01 |
	G:VAL 75	79.36	56.28 |||||||
	G:PRO 76 [H]	95.77	69.60 |||||||
	G:THR 77 [H]	68	51.15 |||||||
	G:ASP 78 [HS]	118.48	77.16 |||||||
	G:PRO 79	81.24	47.21 ||||||
Layer 2	G:CYS 218	14.46	14.30 |||||||||
	G:ALA 219	7.88	3.06 ||||
	G:PRO 220	40.28	11.90 |||
	G:GLN 246	73.11	20.94 |||
	G:CYS 247	30.21	3.47 ||

Light chain		ASA	BSA
CDR L1	L:TYR 32	102.59	62.18 |||||||
CDR L3	L:HIS 90	12.78	8.54 |||||||
	L:LEU 91	71.97	3.85 |
	L:ILE 92	67.24	58.41 ||||||||
	L:GLY 93 [H]	69.62	58.92 ||||||||
	L:LEU 94	135.03	40.24 |||
	L:ARG 96	136.6	19.37 ||

gp120 $_{YU2}$		ASA	BSA
Layer 1	G:PHE 53	126.63	29.22 |||
	G:ALA 60	96.5	34.29 ||||
	G:THR 71 [H]	51.8	31.96 |||||||
	G:HIS 72	148.34	87.07 ||||||
	G:ALA 73	50.7	19.07 ||||
	G:CYS 74	19.79	11.62 ||||||
	G:VAL 75	79.36	23.08 |||
	G:PRO 76	95.77	17.07 ||

ASA Accessible Surface Area, Å²
BSA Buried Surface Area, Å²

2.2c-gp120$_{92UG037}$ core$_e$

Heavy chain		ASA	BSA
	H:GLY 31	29.53	9.21 ||||
	H:TYR 33[H]	63.33	30.11 |||||
CDR H2	H:TRP 47	72.87	11.19 ||
	H:GLU 50	27.06	7.12 |||
	H:LYS 52H	33.55	9.88 |||
	H:SER 56	81.12	8.53 ||
	H:PRO 57[H]	56.57	20.89 ||||
	H:ASN 58[H]	78.33	43.39 ||||||
	H:TYR 59	32.78	2.35 |
	H:HIS 60	51.43	3.93 |
	H:PRO 61	113.57	56.17 |||||
	H:LYS 64	139.32	64.34 |||||
CDR H3	H:ARG 95	33.43	22.79 |||||||
	H:ASN 97[H]	63.59	50.63 ||||||||
	H:TRP 98	201.27	160.32 ||||||||
	H:PRO 99	81.93	2.84 |
	H:LEU 100A	77.89	22.29 |||

gp120$_{92UG037}$		ASA	BSA
Layer 1	A:PHE 53	29.53	9.21 ||||
	A:ALA 58	63.33	30.11 |||||
	A:LYS 59[H]	72.87	11.19 ||
	A:ALA 60[H]	27.06	7.12 |||
	A:TYR 61	33.55	9.88 |||
	A:ASP 62	81.12	8.53 ||
	A:THR 71	56.57	20.89 ||||
	A:VAL 75	78.33	43.39 ||||||
	A:PRO 76H	32.78	2.35 |
	A:THR 77 [H]	51.43	3.93 |
	A:ASP 78[H]	113.57	56.17 |||||
	A:PRO 79	139.32	64.34 |||||
	A:SER 80	33.43	22.79 |||||||
Layer 2	A:CYS 218	63.59	50.63 ||||||||
	A:ALA 219	201.27	160.32 ||||||||
	A:PRO 220	81.93	2.84 |
	A:ALA 221	77.89	22.29 |||
	A:GLN 246	84.86	14.89||

Light chain		ASA	BSA
	L:ILE 2	37.32	17.90 |||||
CDR L1	L:GLN 27	98.92	16.58 ||
	L:GLY 28	50.86	10.89 |||
	L:ILE 29	9.51	0.83 |
	L:TYR 32	89.74	51.02 ||||||
CDR L3	L:HIS 90	6.46	5.56 |||||||||
	L:LEU 91	67.58	3.31 |
	L:ILE 92	72.35	65.84 ||||||||||
	L:GLY 93[H]	42.12	36.14 |||||||||
	L:LEU 94	133.77	31.19 |||
	L:ARG 96	132.91	42.63 ||||

gp120$_{92UG037}$		ASA	BSA
Layer 1	A:PHE 53	114.47	20.66 ||
	A:ALA 60	89.25	37.39 |||||
	A:THR 71[H]	59.08	41.86 ||||||||
	A:HIS 72	163.85	93.17 ||||||
	A:ALA 73	58.99	12.83 |||
	A:CYS 74	27.93	20.89 ||||||||
	A:VAL 75	91.34	42.74 |||||
	A:PRO 76	91.73	25.94 |||

Table S3. Surface area buried at the N5-i5- and 2.2c-gp120 core$_e$ interfaces Buried Surface Area, Å^2 (**BSA**) was calculated using the EBI PISA server (http://www.ebi.ac.uk/msd-srv/prot_int/cgi-bin/piserver).

		mAb N5-i5	mAb 2.2c[a]	mAb 2.2c[b]	mAb 2.2c[c]
Buried Surface Area, Å^2	**gp120 total**	**924**	**902**	**906**	**839.9**
	7-stranded β-sandwich	0	0	21	0
	Layer 1	758	827	853	953
	Layer 2	166	43	29	0
	Layer 3	0	26	3	33
	Heavy chain total	**685**	**632**	**611**	**563**
	CDR H1	84	55	47	45
	CDR H2	372	284	286	183
	CDR H3	229	314	276	273
	Light chain total	**280**	**270**	**251**	**269**
	CDR L1	115	76	62	71
	CDR L2	26	0	0	0
	CDR L3	139	167	189	194
	Heavy and light chain total	965	902	862	865.7

[a]Surface area buried at the 2.2c-gp120$_{89.6P}$ core$_e$ interface of 2.2c Fab- gp120$_{89.6P}$ core$_e$-*d1d2*CD4 complex
[b]Surface area buried at the 2.2c-gp120$_{Yu2}$ core$_e$ interface of 2.2c Fab- gp120$_{YU2}$ core$_e$-M48U1 complex
[c]Surface area buried at the 2.2c-gp120$_{92UG037}$ core$_e$ interface of 2.2c Fab- gp120$_{92UG037}$ core$_e$-M48U1 complex

.

Table S4. Interactions at the N5-i5-gp120$_{93TH057}$ core$_e$ interface. Accessible Surface Area, Å² (**ASA**) and Buried Surface Area, Å² (**BSA**) were calculated using the EBI PISA server (http://www.ebi.ac.uk/msd-srv/prot_int/cgi-bin/piserver). Residues contributing to the interface through H bonds or salt bridges as indicated by a blue letter H or a red letter S, respectively.

Heavy chain		ASA	BSA
CDR H1	H:SER 30	50.95	4.17 |
	H:THR 31	84.14	54.55 |||||||
	H:TYR 32	74.78	14.83 ||
	H:ALA 33	10.17	10.17 ||||||||||
CDR H2	H:ASN 52 H	23.86	22.27 ||||||||
	H:ASN 52A H	70.88	69.50 ||||||||
	H:SER 53	71.9	25.36 ||||
	H:ARG 55 HS	201.78	154.72 ||||||||
	H:ASN 56 H	53.14	49.51 |||||||||
	H:PHE 58	97.84	50.10 ||||||
CDR H3	H:ASP 95	2.97	0.74 |||
	H:LEU 96	118.68	27.01 |||
	H:ARG 97 H	170.51	124.66 ||||||||
	H:LEU 98 H	73.46	66.78 |||||||||
	H:GLY 99	75.43	9.92 ||
gp120 $_{93TH057}$		ASA	BSA
Layer 1	G:THR 51	107.61	39.41 ||||
	G:LEU 52	11.83	10.83 |||||||||
	G:PHE 53	84.15	46.52 ||||||
	G:CYS 54	4.64	4.19 |||||||||
	G:SER 56	5.56	3.31 ||||||
	G:ALA 58	21.05	17.31 ||||||||
	G:LYS 59	99.19	1.66 |
	G:ALA 60	98.42	34.57 ||||
	G:VAL 68	62.35	7.14 ||
	G:TRP 69 H	11.91	9.11 ||||||||
	G:ALA 70	0.53	0.24 |||||
	G:THR 71 H	40.41	36.80 |||||||||
	G:HIS 72 H	167.61	153.94 |||||||||
	G:ALA 73 H	47.78	45.74 |||||||||
	G:CYS 74	12.11	11.86 |||||||||
	G:VAL 75	69.37	33.83 |||||
	G:PRO 76	115.55	42.00 ||||
Layer 2	G:GLN 103 H	25.5	12.29 |||||
	G:GLU 106	116.61	23.39 |||
	G:ASP 107 HS	38.17	33.85 |||||||||
	G:SER 110	52.38	22.41 |||||
	G:GLN 114 H	92.88	50.21 ||||||
	G:TYR 217	0.91	0.44 |||||

Light chain		ASA	BSA
CDR L1	L:SER 29	64.81	32.59 ||||||
	L:TYR 30	65.08	50.04 ||||||||
	L:PHE 32	113.12	32.42 |||
CDR L2	L:TYR 49	76.81	1.57 |
	L:GLU 50	80.79	25.53 ||||
CDR L3	L:TYR 91	62.07	42.42 |||||||
	L:GLY 93	15.4	4.18 |||
	L:SER 94	101.13	52.42 ||||||
	L:THR 95	130.95	22.56 ||
	L:PHE 95B	116.12	16.98 ||
gp120 $_{93TH057}$		ASA	BSA
Layer 2	G:PHE 53	84.15	29.66 ||||
	G:ALA 58	21.05	3.74 ||
	G:ALA 60	98.42	24.91 |||
	G:HIS 61	153.89	3.41 |
	G:VAL 75	69.37	35.54 ||||||
	G:PRO 76	115.55	73.56 |||||||
	G:THR 77	46.32	6.39 ||
	G:ASP 78	94.03	27.73 |||
	G:PRO 79	125.58	52.36 |||||
	G:ASN 80	107.69	2.09 |
	G:THR 219	11.3	0.86 |
	G:ALA 221	98.47	22.19 |||

ASA Accessible Surface Area, Å²
BSA Buried Surface Area, Å²

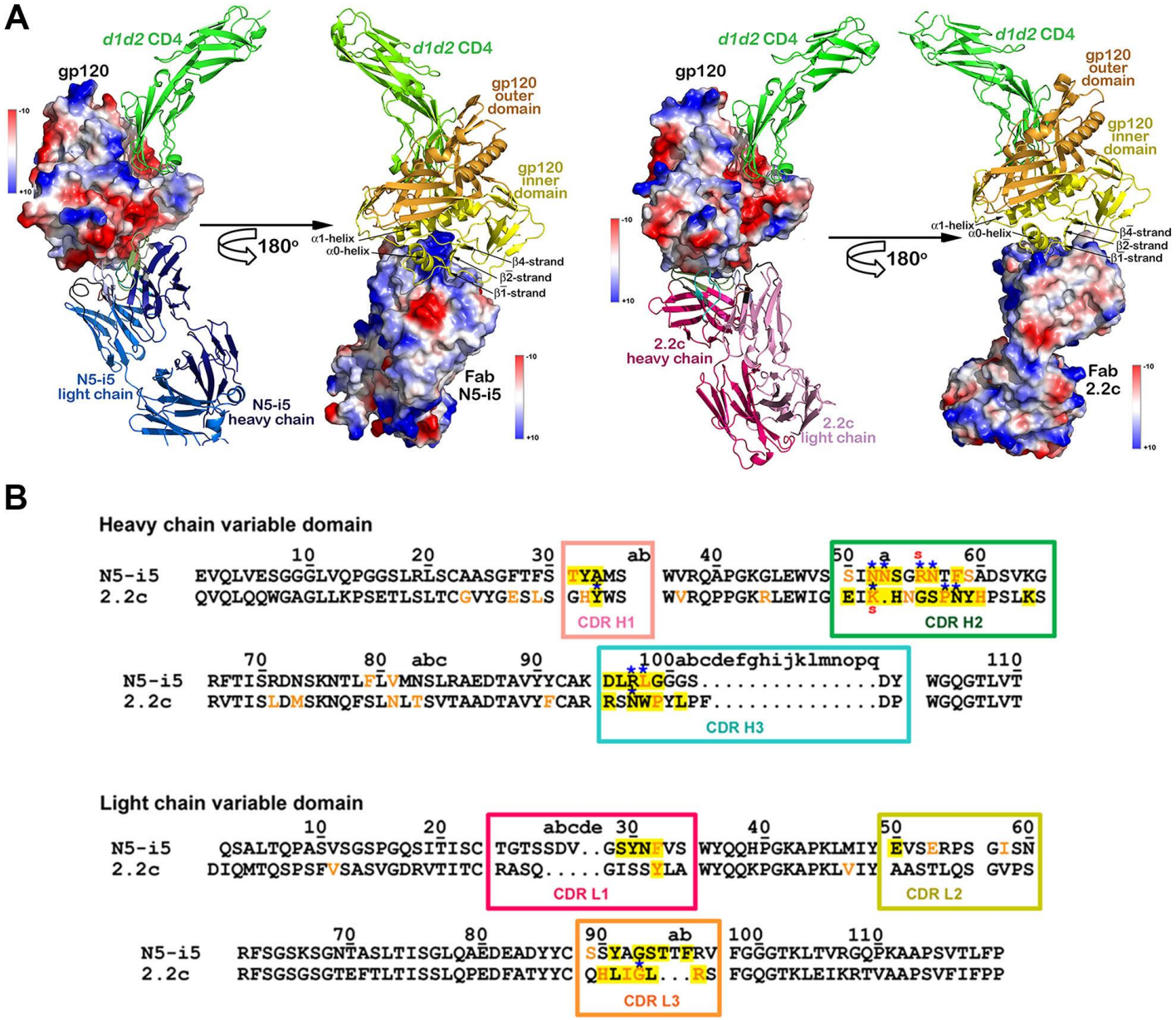

Figure S1. Crystal structures of N5-i5 Fab-gp120$_{93TH057}$ core$_e$-*d1d2*CD4 and 2.2c Fab-$_{gp12089.6P}$ core$_e$-*d1d2*CD4 complex. (A) Structures were aligned based on the gp120 molecule and are shown as the ribbon diagrams (with the electrostatic potential displayed at the gp120 molecular surfaces and a 180^o view about a vertical axis with electrostatic potential displayed at the Fab molecular surfaces. The electrostatic potential is colored red for negative, blue for positive and white for apolar. The structural gp120 elements engaged in mAbs binding – the β2-, β1-, β4-strand, the α0-helix and the α1-helix – are labeled. (**B**) Alignment of mAb N5-i5 and 2.2c sequences and contact residue mapping. Sequences of the heavy and light chains of Fabs are aligned and residues buried upon gp120 complex formation are highlighted in yellow. Residues contributing to the binding through H bonds or salt bridges are indicated by blue asterisks or red lower case letters above the mAb sequence, respectively. Complementarity-determining regions (CDRs) on the heavy chain and the light chain of the variable regions are marked by colored boxes: CDR H1-salmon, CDR H2-green, CDR H3-cyan, CDR L1-magenta, CDR L2-yellow, CDR L3-orange. Residues subjected to the somatic mutation from the germline sequences are highlighted in orange. Kabat numbering of antibody sequences is applied throughout (3). Six CDRs are involved in forming the binding site on mAb N5-i5. CDR H2 is central to the binding, burying 372 Å^2 at the complex interface (Table S3). Out of six residues of CDR H2 (residues 52-53, 55-56 and 58) engaged in gp120 binding, four are involved in H-bonds and ionic interactions. An additional two H-bonds are

formed by the Arg^{97} and Leu^{98} of CDR H3, which contribute residues 95-99 to the complex interface and bury an additional 229 $Å^2$ surface area. The structure of N5-i5 Fab-$gp120_{93TH057}$ $core_e$-*d1d2*CD4 determined at high resolution indicate also the possible water-mediated H-bonds engaging residues of CDR H2 and CDR H3. The rest of the energy of binding is provided by residues 29-32 (CDR L1), 50 (CDR L2), 91, 93-95, 95B (CDR L3) of the light chain and 31-33 (CDR H1) of the heavy chain, which all contribute exclusively through hydrophobic forces (Table S3-S4). All residues of N5-i5 CDR H2 involved in specific interactions with gp120 antigen were subjected to the somatic mutation from the germline sequences.

The contact area assembled of five CDRs, three from the heavy chain (residues 50, 52-54 of CDR H1; 56-61, 64 of CDR H2; 95, 97-99, 100A of CDR H3) and two from the light chain (residues 32 of CDR L1 and 90-94, 96 of CDR L3) form the binding site of mAb 2.2c. The CDR L2 provides no contacts to the ligand. The CDR H3 and H2 (286 and 278 $Å^2$ surface area buried, respectively, Table S3) of mAb 2.2c play a central role in gp120 $core_e$ binding through contact interactions (van der Waals forces), H-bonds and ionic interactions, while the rest makes considerably fewer contacts with the antigen. A total of eight H-bonds an one salt bridge are formed at the mAb 2.2c–Core interface contributed by Tyr^{33} of CDR H1, Lys^{52}, Pro^{57} and Asn^{58} of CDR H2, Asn^{97} of CDR H3 and Gly^{93} of CDR L3 (Table S2). CDR L3 of mAb 2.2c interacts with the gp120 antigen exclusively through van der Waals contacts (Table S2-S3).

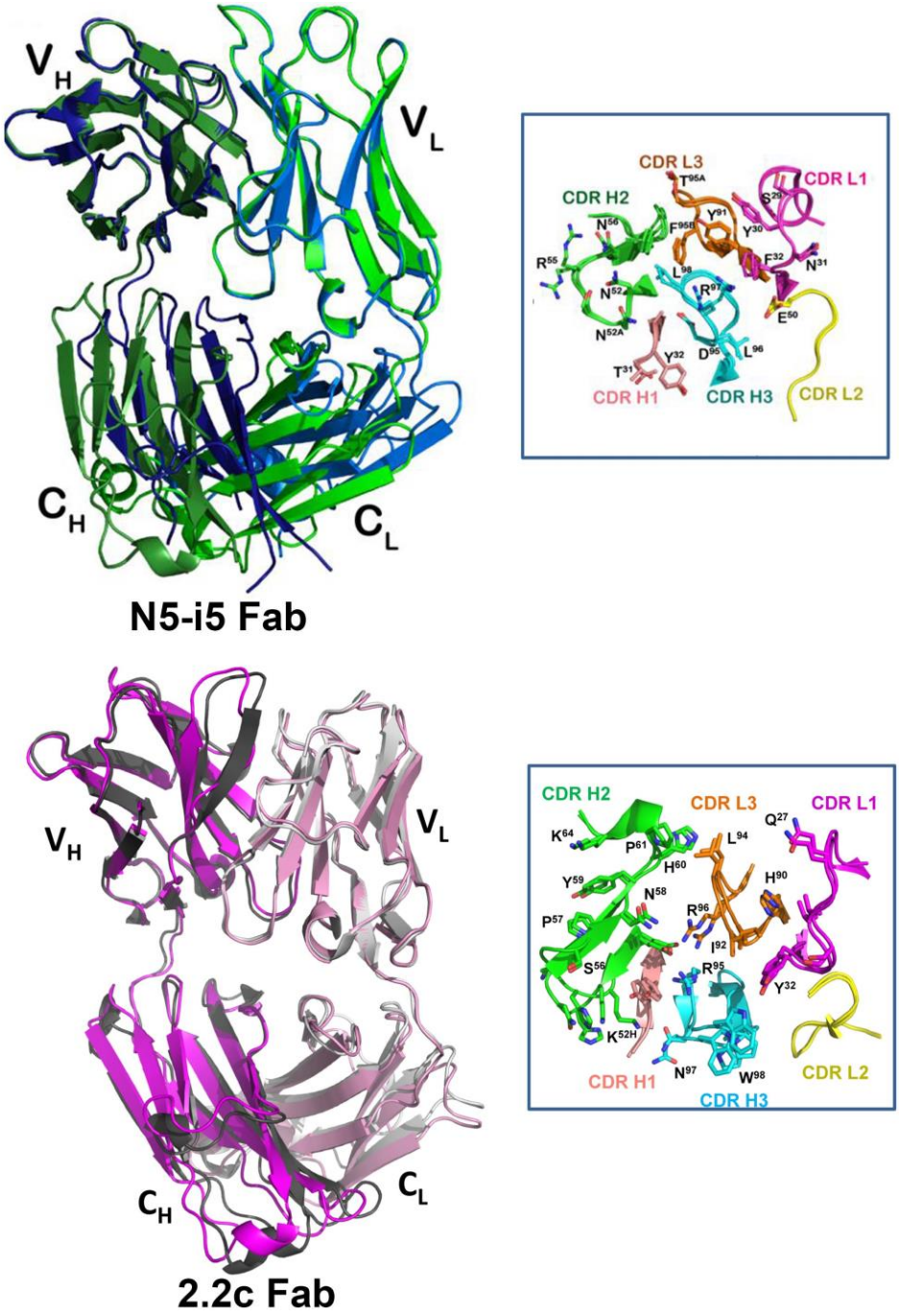

Figure S2. Free versus gp120-bound states of N5-i5 and 2.2c Fab. Ribbon diagram is shown of superposition of the structures of N5-i5 Fab (PDB: 3TNN4, dark green-heavy chain and light green-light chain) and 2.2c Fab (dark grey-heavy chain and light grey-light chain) alone and N5-i5 Fab (dark blue-heavy chain and light blue-light chain) and 2.2c Fab (dark magenta-heavy chain and light magenta-light chain) bound to CD4-triggered gp120. The VH-VL domains were superimposed to show movement of the constant domains. Close-up views show Fab combining sites in their free and bound conformations. Only residues contributing to gp120 binding of the Fab combining site are shown and displayed as balls-and-sticks. CDRs are colored in magenta (CDR L1), yellow (CDR L2), orange (CDR L3), salmon (CDR H1), green (CDR H2), and cyan (CDR H3).

Only marginal adjustments of the side chains within the CDRs of N5-i5 and 2.2c Fab occur upon gp120 binding. The most noticeable difference is observed in the relative orientation of the constant and variable domains, where Fab in the bound conformation adopts a more acute elbow bend angle. This mode of interaction, which requires limited conformational shift upon ligand binding, fits a lock-and-key model with minimal induced fit.

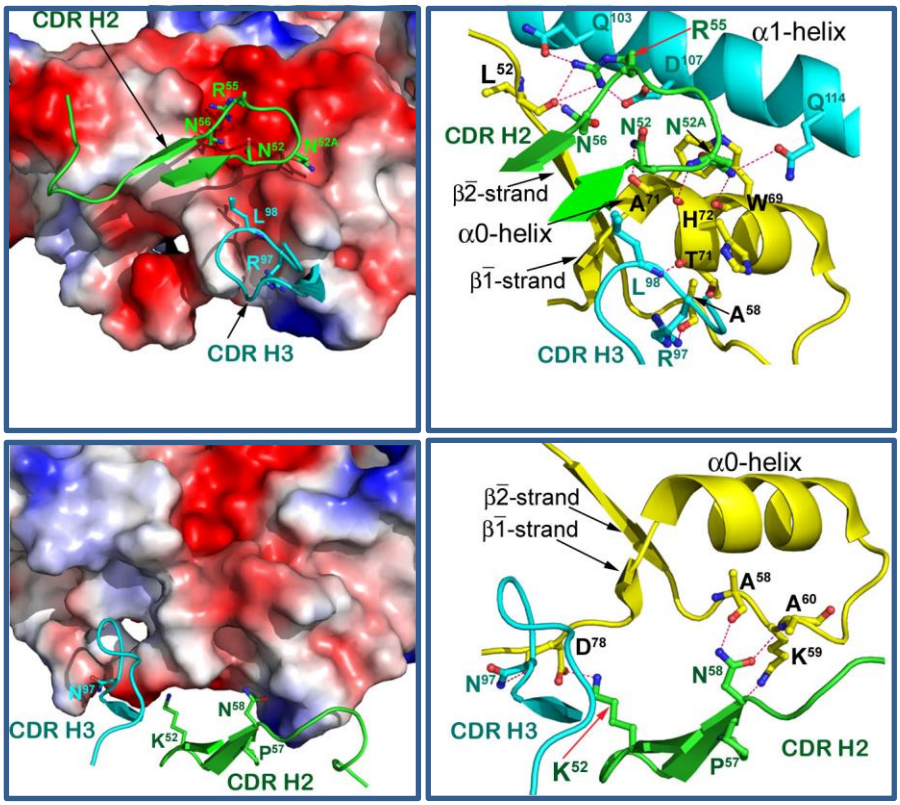

Figure S3. Close-up views of binding interfaces of CDR H2 and CDR H3 loops of mAb N5-i5 (top) and mAb 2.2c (bottom) with gp120. Antibody complementary determining region residues engaged in gp120 binding are shown as balls-and-sticks. The electrostatic potential of gp120 is displayed over its molecular surface. H-bonds are shown as dashes in magenta.

In the mAb N5-i5-gp120$_{93TH057}$ core$_e$ complex, Asn^{52A} and Arg^{55} are located in a center interaction network which pins the CDR H2 of the antibody to the α1-helix of layer 2. They anchor the conserved electronegative patch formed by Gln^{103}, Glu^{106}, Asp^{107} and Gln^{114} at the α1-helix and establish an Arg^{55}-Asp^{107}$_{gp120}$ salt bridge and a number of direct and water-mediated H-bonds (Table S4). In parallel, the CDR H2 contacts layer 1, with Asn^{52}, Asn^{52A} and Asn^{56} establishing multiple H-bonds with residues clustered around the α0-helix and the β$\bar{2}$ strand. On CDR H3, two H-bonds are formed involving Arg^{97} and Leu^{98} of the antibody.

The binding mode of mAb 2.2c enables its contacts with the α1-helix of layer 2. CDR H2 of 2.2c binds a negative gp120 surface within layer 1 clustered around the loops connecting the α0-helix to the β$\bar{1}$-strand and the β$\bar{1}$- to the β0-strand of gp120. Three H-bonds are formed involving Pro^{57} Asn^{58} of CDR H2 and Lys^{59} and Ala^{58} and Ala^{60} of layer 1. In addition Lys^{52} of CDR H2 establishes a salt bridge and a hydrogen bond, via the ε-NH3(+) group of and the Asp^{78} the loop connecting β$\bar{1}$- to the β0-strand of gp120. CDR H3 establishes contact with layer 1 via a H-bond formed by the side chain nitrogen of Asn^{97} and Asp^{78} O of gp120 (Table S2).

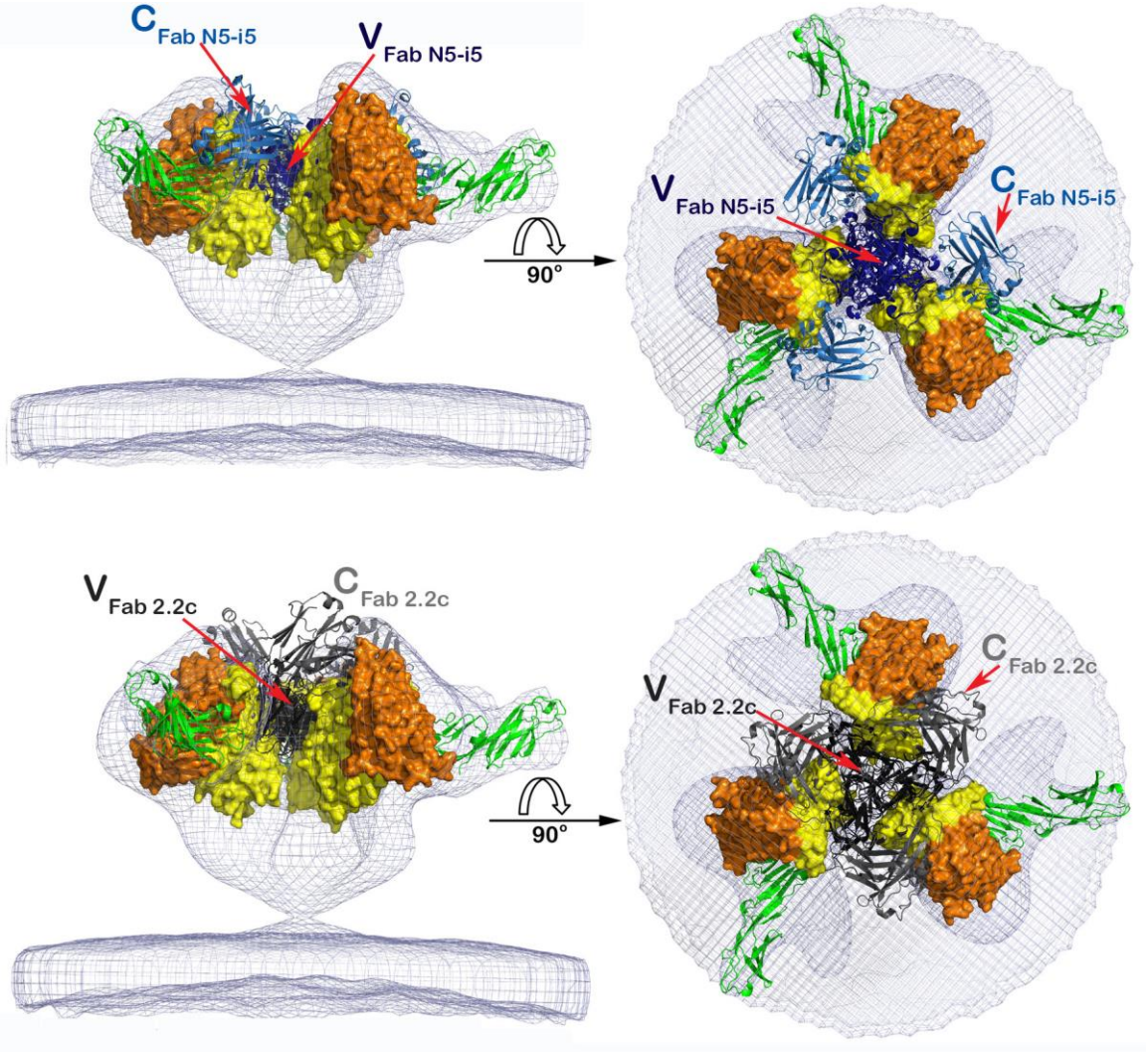

Figure S4. Fitting of the N5-i5 Fab-gp120$_{93TH057}$-*d1d2*CD4 (top) and 2.2c Fab-gp120$_{89.6P}$-d1d2CD4 (bottom) structures into maps of gp120$_{Bal}$-*d1d2*CD4 complex derived by cryoelectron tomography(4). The X-ray coordinates for mAb N5-i5- and 2.2 complexes were fitted into gp120$_{Bal}$-*d1d2*CD4 tomograms using the program Chimera (5). All molecules but gp120 (represented by molecular surfaces) are shown as ribbon diagrams. The gp120 inner domain is shown in yellow, the outer domain in orange, *d1d2*CD4 in green and the cryo-EM density map in grey. The variable and constant domains of N5-i5 Fab and 2.2c Fab are shown in dark and light blue and gray, respectively. The views of trimers are from the side with the viral membrane orientated toward the bottom (left panel) and rotated 90^{o} about a horizontal axis with the viral membrane at the bottom (right panel).

When the N5-i5 and 2.2c Fab-bound complexes are fitted into the gp120$_{Bal}$-*d1d2*CD4 trimers the variable domains of mAb overlay entirely and occupy the presumable position of the gp41 within the trimer. Multiple crushes occur between the constant part of mAb and the gp120 component of trimer confirming that these antibodies are unable to reach their gp120 binding sites within gp120$_{Bal}$-*d1d2*CD4 spike.

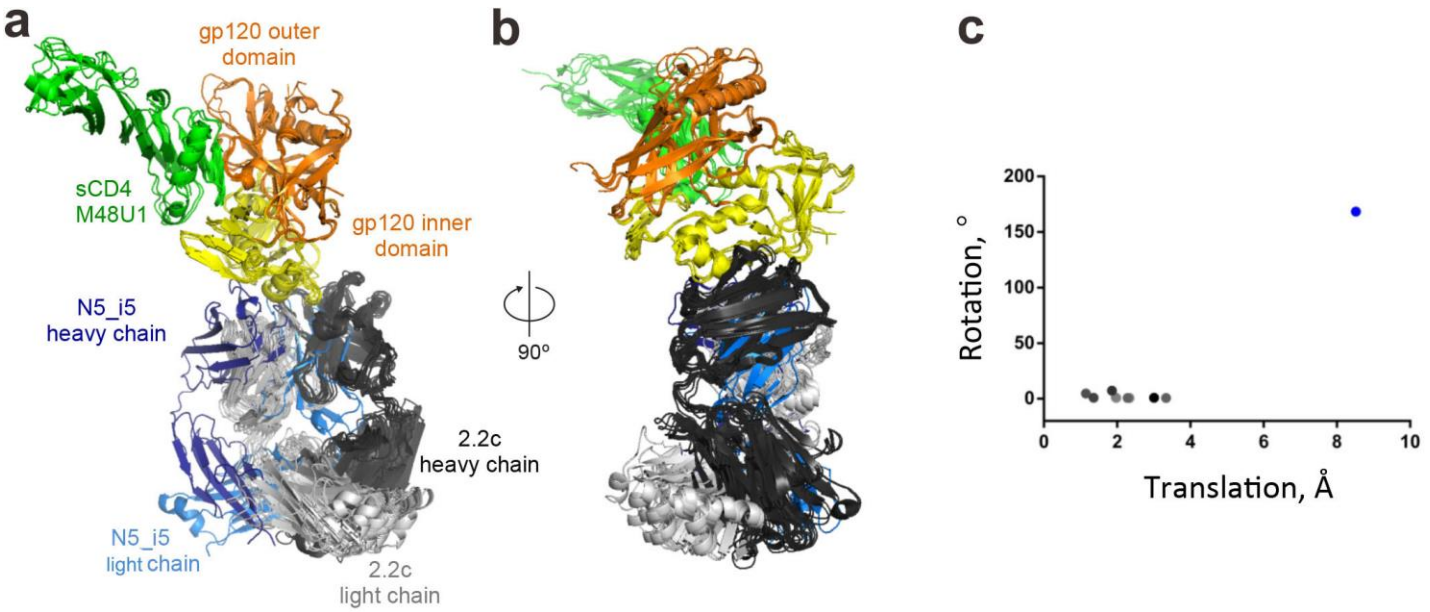

Figure S5. Relative orientation of mAb N5-i5 and 2.2c in their complexes with gp120. (**A**) Superimposition of the N5-i5 Fab-gp120$_{93TH057}$ core$_e$-*d1d2*CD4 complex and the 2.2c-bound complexes from three crystal structures: 2.2c Fab- gp120$_{89.6P}$ dV1V2-*d1d2*CD4 (1 complex in ASU), 2.2c Fab- gp120$_{YU2}$ core$_e$-M48U1 (1 complex in ASU) and 2.2c Fab- gp120$_{92UG037}$ core$_e$-M48U1 (8 complexes in ASU). Structures were aligned based on the gp120 outer domain in each complex. The gp120 inner domain is shown in yellow and the outer domain in dark orange. The N5-i5 Fab and 2.2c Fab is shown in blue and gray, respectively, with the heavy chain of each colored in a darker shade than the light chain. sCD4 and M48U1 are colored green. (**B**) 90° rotated view from (A). (**C**) Rotation and translation plots showing the relative orientations of 2.2c and N5-i5 Fabs in the different crystal complexes. The relative orientations were quantified by first superimposing the complexes based on the gp120 outer domain as shown in (A) and (B). Next, the 2.2c Fab- gp120$_{YU2}$ core$_e$-M48U1 complex was chosen as the reference, and the Fabs in all other complexes were aligned to the 2.2c Fab of this complex based on the VH framework regions. The rotation and translation required to align each antibody with the reference antibody are a measure of the relative orientations in their respective complexes. The 2.2c data points are colored in varying shades of grey with each shade indicating a different complex. The N5-i5 data point is colored blue.

The binding orientation of 2.2c (grey dots) was preserved in all three complexes with different gp120 strains and crystal lattices, whereas Fab N5-i5 (blue dot) needs to be rotated about 160° and translated ~8 Å from its binding orientation in its complex with gp120, to align with the reference 2.2c Fab in the Fab 2.2c-gp120$_{YU2}$-M48U1 complex.

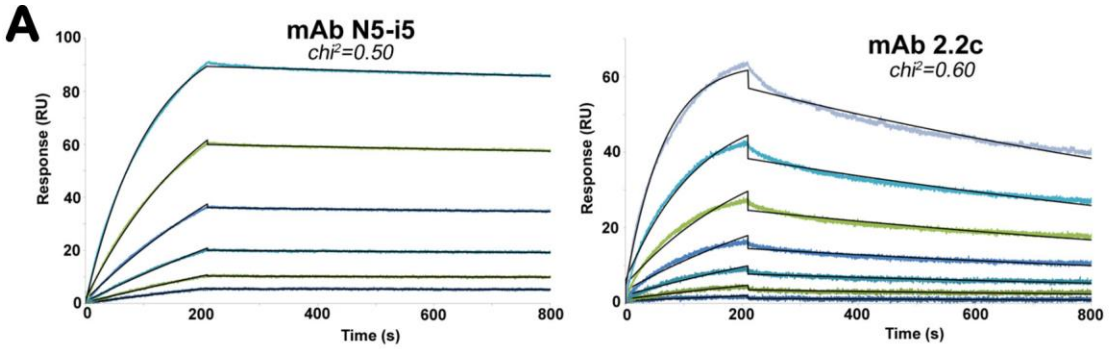

	mAb N5-i5	mAb 2.2c	fold*
K_d (M)	$2.7\pm1.6 \times 10^{-10}$	$4.9\pm 0.5 \times 10^{-10}$	1.8
k_a (1/Ms)	$6.7\pm0.5 \times 10^{5}$	$11.5\pm1.3 \times 10^{5}$	1.7
k_d (1/s)	$19.6\pm6.2 \times 10^{-5}$	$55.6\pm12.5 \times 10^{-5}$	2.8

* fold difference

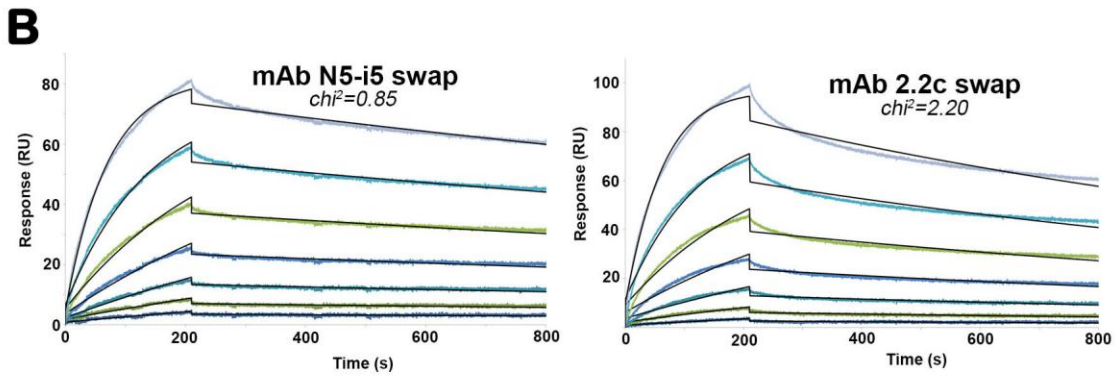

	mAb N5-i5	mAb N5-i5 swap	Fold change[1]	mAb 2.2c	mAb 2.2c swap	Fold change[1]
K_d (M)	$2.7 \pm 1.6 \times 10^{-10}$	$3.2 \pm 0.3 \times 10^{-10}$	**1.2**	$4.9 \pm 0.5 \times 10^{-10}$	$4.9 \pm 0.2 \times 10^{-10}$	**1.0**
k_a (1/Ms)	$6.7 \pm 0.45 \times 10^{5}$	$12.0 \pm 0.4 \times 10^{5}$	**1.8**	$11.5 \pm 1.3 \times 10^{5}$	$13.5 \pm 1.1 \times 10^{5}$	**1.2**
k_d (1/s)	$19.6 \pm 6.2 \times 10^{-5}$	$38.5 \pm 4.4 \times 10^{-5}$	**2.0**	$55.6 \pm 12.5 \times 10^{-5}$	$66.4 \pm 2.6 \times 10^{-5}$	**1.2**

[1] relative to the wild type mAb

Figure S6. Binding of mAb N5-i5 and mAb 2.2c (A) and their Fv-swapped variants (B) to a single-chain gp120Bal-CD4 complex (FLSC[22]) as measured by SPR. Protein A was covalently bound to individual flow cell surfaces of a CM5 sensor chip with amine-coupling method Antibodies were captured onto protein A surfaces to a specific level at about 150 RU. For kinetic measurement of the single-chain gp120BaL-CD4 complex (FLSC (53)) binding to immobilized antibody, sensorgrams were obtained by passing various concentrations of FLSC (0-200 nM). A buffer injection served as a negative control. Upon completion of each association and dissociation cycle, surfaces were pulsed with regeneration solution. The data were double referenced by subtraction of the blank surface (no antibody) and a blank injection (no analyte). Binding curves were globally fit to a 1:1 binding model. The experiments were repeated with similar results. The binding kinetics (association rates (k_a), dissociation rates (k_d), and affinity constants (K_d)) were calculated with the BIAevaluation software.

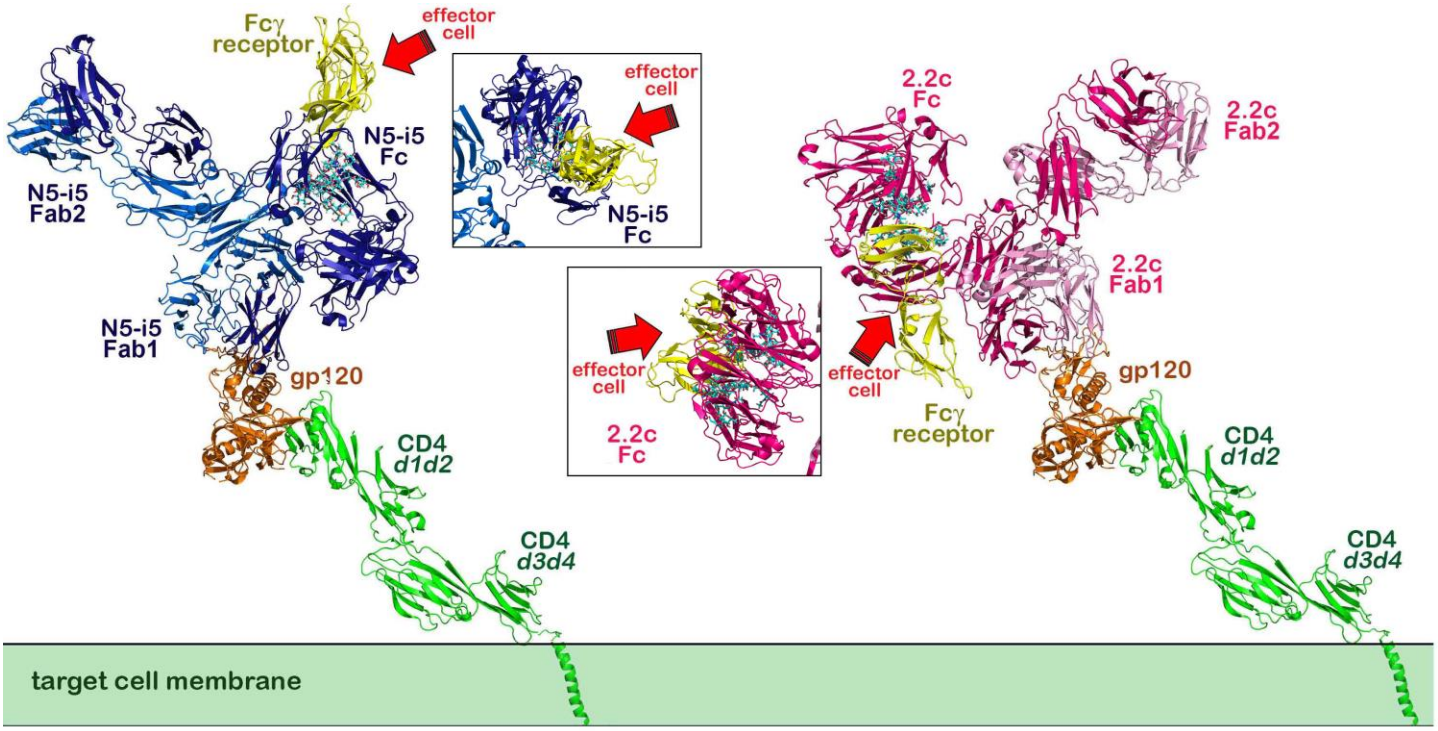

Figure S7. Models of putative ADCC immune-complexes formed by mAb N5-i5 and 2.2c at the target/effector cell interface. The four-domain CD4 (shown in green) was generated by superimposing structure of four domain CD4 (*d1-d4*CD4, residues 1 to 363, PDB code: 1WIO (6)) onto *d1d2* domains of determined structures of the N5-i5Fab-gp120$_{93TH057}$core$_e$-*d1d2*CD4 and 2.2cFab-gp120core$_{89.6P}$-*d1d2*CD4. The complexes were superimposed based on gp120 molecule (shown in orange), oriented relative to the target cell membrane by modeling the CD4 transmembrane domain (PDB code: 2KLU (7)). Next, structure of monoclonal murine antibody subclass IgG1 (PDB code 1IGY (8)) was superimposed onto Fab molecule of each Fab-gp120-*d1d4*CD4 model. IgG heavy/light chain are colored dark/light blue and pink for N5-i5 and 2.2c, respectively. At the end, the human FcγRIII receptor (the extracellular part residues 1–172) was added by overlaying the Fc-FcγRIII complex (PDB code 1E4K (9)) onto Fc domain of intact IgG. From two possible orientations of FcγRIII within the Fc-FcγRIII complex (10) the one with no direct steric conflict with the hinge region and Fab was selected (*d1d2* domains, shown in yellow). Complexes were assembled assuming monovalent binding of mAb through Fab1 and Fab2 (shown in inlets as close-up view into Fc regions only). Portion of the human Fcγ receptor as bound to Fc regions of mAbs indicate the putative position of the effector cell and red arrows indicate the angle of the attack by which the effector cell needs to target Fc region of each mAb.

Two slightly different positions of the human Fcγ receptor within the immune complexes of each mAb are modeled depending which Fab arm of IgG1 is involved in the binding to CD4-triggered gp120. In both modes of attachment N5-i5 faces its FcR binding domain away from the target cell surface while 2.2c positions its FcR binding domain toward the target cell surface. However, the mode of N5-i5 and 2.2c binding through Fab2 reveals a less pronounced difference in the angle of attack by which the effector cell needs to target Fc region. This suggests that in addition to relative orientation of the reactive site on the Fab, other steric parameters of IgG influence the geometry of the immune complexes. It is known that the hinge region flexibility of IgG, as demonstrated by hinge bending, wagging and torsional rotation/translation, affects the geometry of immune complexes at the target/effector cell interface in a way that is largely understudied (11, 12). The crystallographic murine IgG1 structure (8) used here as a template samples to some extend the hinge-folding mode of flexibility of IgG1 as shown by its distorted Y shape with two different hinge region angles: Fc-Fab1 of 78˚ and Fc-Fab2 of 123˚. Given that the "preferred" (mean) Fab-Fc angle of human IgG1 is 107˚ with the standard deviation value (hinge-folding flexibility) of ±30˚(11) the Fc region of 2.2c most likely will be positioned in the immune complex less favorably for Fcγ receptor interaction as compared to N5-i5.

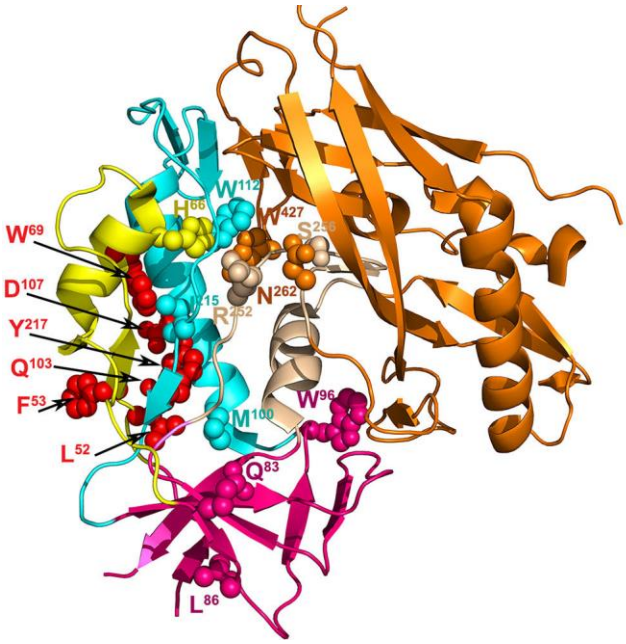

gp120 residue	N5-i5 contacts	2.2c contacts	Layer	ref (13)	ref (14, 15)
52	Yes	No	1	ND	+
53	Yes	Yes	1	ND	+
66	No	No	1	ND	+
69	Yes	No	1	+	+
83	No	No	7-stranded-β sandwich	ND	+
86	No	No	7-stranded-β sandwich	ND	+
96	No	No	7-stranded-β sandwich	ND	+
100	No	No	2	ND	+
103	Yes	No	2	ND	+
107	Yes	No	2	ND	+
112	No	No	2	ND	+
215	No	No	2	ND	+
217	Yes	No	2	ND	+
252	No	No	3	+	ND
256	No	No	3	+	ND
262	No	No	Outer Domain	+	ND
427	No	No	β20-β21 loop	+	+

ND, not done
+, binding affected

Figure S8. N5-i5 and 2.2c contact residues versus residues affecting mAb A32 binding to gp120. Residues shown by mutagenesis studies (13-15) to affect binding of mAb A32 to gp120 Env are shown as spheres and colored in inner domain color scheme. N5-i5 and 2.2c contact residues that overlap the residues shown to affect A32 binding are shown in red. The first column in the chart lists 17 residues shown to affect A32 binding in prior mutagenesis studies. The second and third columns denote whether the residues are also contact residues for N5-i5 and 2.2c, respectively.

Supplemental References

1. **Brunger AT.** 1992. Free R value: a novel statistical quantity for assessing the accuracy of crystal structures. Nature **355:**472-475.
2. **Chen VB, Arendall WB, 3rd, Headd JJ, Keedy DA, Immormino RM, Kapral GJ, Murray LW, Richardson JS, Richardson DC.** 2010. MolProbity: all-atom structure validation for macromolecular crystallography. Acta crystallographica. Section D, Biological crystallography **66:**12-21.
3. **Kabat EA.** 1976. Structure of antibody combining sites. Ann Immunol (Paris) **127:**239-252.
4. **Tran EE, Borgnia MJ, Kuybeda O, Schauder DM, Bartesaghi A, Frank GA, Sapiro G, Milne JL, Subramaniam S.** 2012. Structural Mechanism of Trimeric HIV-1 Envelope Glycoprotein Activation. PLoS Pathog **8:**e1002797.
5. **Pettersen EF, Goddard TD, Huang CC, Couch GS, Greenblatt DM, Meng EC, Ferrin TE.** 2004. UCSF Chimera--a visualization system for exploratory research and analysis. Journal of computational chemistry **25:**1605-1612.
6. **Wu H, Kwong PD, Hendrickson WA.** 1997. Dimeric association and segmental variability in the structure of human CD4. Nature **387:**527-530.
7. **Wittlich M, Thiagarajan P, Koenig BW, Hartmann R, Willbold D.** 2010. NMR structure of the transmembrane and cytoplasmic domains of human CD4 in micelles. Biochimica et biophysica acta **1798:**122-127.
8. **Harris LJ, Skaletsky E, McPherson A.** 1998. Crystallographic structure of an intact IgG1 monoclonal antibody. J Mol Biol **275:**861-872.
9. **Sondermann P, Huber R, Oosthuizen V, Jacob U.** 2000. The 3.2-A crystal structure of the human IgG1 Fc fragment-Fc gammaRIII complex. Nature **406:**267-273.
10. **Radaev S, Motyka S, Fridman WH, Sautes-Fridman C, Sun PD.** 2001. The structure of a human type III Fcgamma receptor in complex with Fc. J Biol Chem **276:**16469-16477.
11. **Roux KH, Strelets L, Michaelsen TE.** 1997. Flexibility of human IgG subclasses. J Immunol **159:**3372-3382.
12. **Saphire EO, Stanfield RL, Crispin MD, Morris G, Zwick MB, Pantophlet RA, Parren PW, Rudd PM, Dwek RA, Burton DR, Wilson IA.** 2003. Crystal structure of an intact human IgG: antibody asymmetry, flexibility, and a guide for HIV-1 vaccine design. Adv Exp Med Biol **535:**55-66.
13. **Moore JP, McCutchan FE, Poon SW, Mascola J, Liu J, Cao Y, Ho DD.** 1994. Exploration of antigenic variation in gp120 from clades A through F of human immunodeficiency virus type 1 by using monoclonal antibodies. J Virol **68:**8350-8364.
14. **Finzi A, Xiang SH, Pacheco B, Wang L, Haight J, Kassa A, Danek B, Pancera M, Kwong PD, Sodroski J.** 2010. Topological layers in the HIV-1 gp120 inner domain regulate gp41 interaction and CD4-triggered conformational transitions. Mol Cell **37:**656-667.
15. **Veillette M, Desormeaux A, Medjahed H, Gharsallah NE, Coutu M, Baalwa J, Guan Y, Lewis G, Ferrari G, Hahn BH, Haynes BF, Robinson JE, Kaufmann DE, Bonsignori M, Sodroski J, Finzi A.** 2014. Interaction with Cellular CD4 Exposes HIV-1 Envelope Epitopes Targeted by Antibody-Dependent Cell-Mediated Cytotoxicity. J Virol **88:**2633-2644.